

Crystal structure, Hirshfeld surface analysis and energy framework study of 6-formyl-7,8,9,11-tetrahydro-5H-pyrido[2,1-b]quinazolin-11-one

Akmal Tojiboev,^{a*} Sherzod Zhurakulov,^{b,c} Valentina Vinogradova,^b Ulli Englert^d and Ruimin Wang^d

Received 19 November 2020

Accepted 9 December 2020

Edited by M. Weil, Vienna University of Technology, Austria

Keywords: Tricyclic quinazoline derivative; intramolecular N—H···O bond; π – π interactions; Hirshfeld surface analysis; energy frameworks; crystal structure.

CCDC reference: 2049242

Supporting information: this article has supporting information at journals.iucr.org/e

^aArifov Institute of Ion-Plasma and Laser Technologies of Uzbekistan Academy of Sciences, 100125, Durmon Yuli St. 33, Tashkent, Uzbekistan, ^bS. Yunusov Institute of Chemistry of Plant Substances, Academy of Sciences of Uzbekistan, Mirzo Ulugbek Str. 77, 100170 Tashkent, Uzbekistan, ^cNational University of Uzbekistan named after Mirzo Ulugbek, 100174, University Str. 4, Olmazor District, Tashkent, Uzbekistan, and ^dInstitute of Inorganic Chemistry, RWTH Aachen University, Landoltweg 1, 52056 Aachen, Germany. *Correspondence e-mail: a_tojiboev@yahoo.com

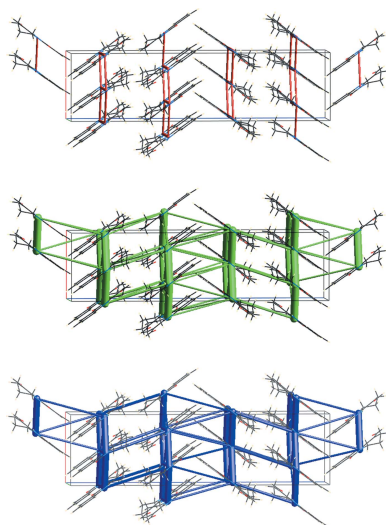
At 100 K, the title compound, C₁₃H₁₂N₂O₂, crystallizes in the orthorhombic space group *Pna*2₁ with two very similar molecules in the asymmetric unit. An intramolecular N—H···O hydrogen bond leads to an *S*(6) graph-set motif in each of the molecules. Intermolecular π – π stacking and C=O··· π interactions involving the aldehyde O atoms link molecules into stacks parallel to [100]. A Hirshfeld surface analysis indicates that the most important contributions to the crystal packing stem from H···H (49.4%) and H···O/O···H (21.5%) interactions. Energy framework calculations reveal a significant contribution of dispersion energy. The crystal studied was refined as a two-component inversion twin.

1. Chemical context

Two major aspects contribute to the interest in modified structural analogues of quinazoline alkaloids. On the one hand, they are attractive targets for the development of methods in organic synthesis; reactions sufficiently general to target a wide range of derivatives of a given lead structure should be easy to carry out and warrant high yields. On the other hand, substituted quinazolines allow the study of structure–property relationships with respect to their biological activities (Shakhidoyatov, 1988; Shakhidoyatov & Elmuradov, 2014).

The quinazoline alkaloid 7,8,9,11-tetrahydro-5H-pyrido[2,1-*b*]quinazolin-11-one (mackinazolinone alkaloid) was first isolated from the plant *Mackinlaya subulata* Philipson (Fitzgerald *et al.*, 1966). A simple method for the synthesis of mackinazolinone *via* condensation of anthranilic acid with δ -valerolactam promoted the use of this compound as a synthon for chemical transformations (Shakhidoyatov *et al.*, 1976; Oripov *et al.*, 1979).

The title compound, 6-formyl-7,8,9,11-tetrahydro-5H-pyrido[2,1-*b*]quinazolin-11-one (**1**) (Fig. 1), does react with primary amines (Zhurakulov & Vinogradova, 2015, 2016), but does not react with pseudoephedrine or 1-(phenyl)-6,7-dimethoxy-1,2,3,4-tetrahydroisoquinoline in a range of solvents with different polarities such as acetonitrile, chloroform, ethanol, trifluoroacetic acid, acetic acid, benzene, DMF



OPEN ACCESS

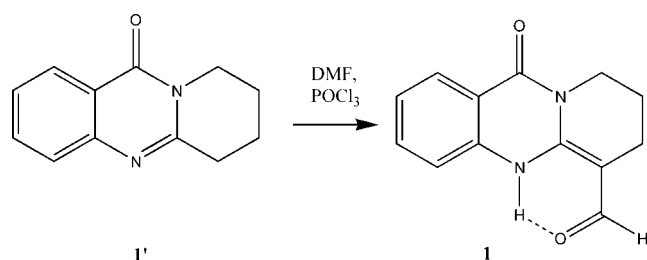
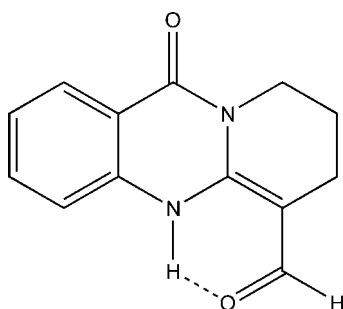


Figure 1
Chemical scheme showing the synthesis of the title compound.

or dioxane. The existence of several tautomeric forms for compound (**1**) may be the reason for this selectivity towards primary amines.

Based on ^1H NMR data and quantum-chemical calculations, Zhurakulov *et al.* (2016) confirmed that the tautomer with the intramolecular hydrogen bond represents the energetically favourable form. In order to establish the tautomeric form of (**1**) in the solid state, we studied its molecular and crystal structure. We also report the analysis of the Hirshfeld surface and the energy framework of crystalline (**1**).



2. Structural commentary

The asymmetric unit of the title compound contains two molecules *A* and *B* (Fig. 2). They are almost superimposable, with an r.m.s. of 0.023 Å (Spek, 2020); an overlay of *A* and *B* is depicted in the supporting information (Fig. S1). In contrast to the quinazolinone moiety, the alkyl ring is not planar. The maximum deviation from the least-squares plane through each of the molecules is encountered for the atoms C2*A* and C2*B*

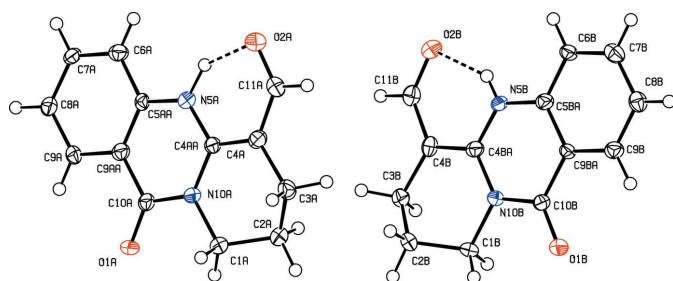


Figure 2
The asymmetric unit of (**1**) with the atom-numbering scheme. Displacement ellipsoids are drawn at the 50% probability level. The intramolecular N—H...O hydrogen bond forming an *S*(6) ring motif is shown with dashed lines.

and amounts to 0.515 (3) and 0.521 (3) Å, respectively. The almost coplanar arrangement of the aldehyde group and the pyrimidine ring in either molecule *A* and *B* enables an intramolecular N—H...O interaction (Table 1) and formation of an *S*(6) graph-set motif.

Molecules of (**1**) stack into columns parallel to [100] in an equidistant series of coplanar moieties; the independent molecules *A* and *B* segregate into different stacks (Fig. 3). The intra-stack arrangement does obviously not correspond to translation but involves the *a* glide plane with its mirror component along [010]. The carbonyl groups in subsequent molecules of a stack are therefore oriented alternately in the positive and negative direction of the crystallographic *b* axis, and the same arrangement can be expected for their dipole moments. Although no ‘real’ translation relates consecutive molecules along [100], the rather regular arrangement of essentially planar objects at half a lattice parameter is reflected in moderate pseudosymmetry in reciprocal space: reflection intensities I_{hkl} are stronger for even indices *h* than for odd ones, with a ratio $I_{hkb} h = 2n : I_{hkb} h = (2n + 1)$ of 1.5.

Compound (**1**) crystallizes in the non-centrosymmetric achiral space group *Pna*2₁, and its absolute structure deserves a comment. The absolute structure is linked to the direction of the polar screw axis along [001]. In the absence of heavy atoms, resonant scattering in (**1**) is minor, with *Friedif* (Flack & Shmueli, 2007) of 28. We have recently investigated a case of similar low resonant scattering in a Sohnke group, where the absolute structure could be linked to the absolute configuration of the target molecule, and chemical and spectroscopic information could help (Wang & Englert, 2019). As might be expected, the commonly used indicators for diffraction-based assignment of the absolute structure of (**1**) were associated with rather large standard uncertainties: the Flack parameter (Flack, 1983) refined to 0.51 (7), and similar results were obtained for Parsons’ quotient method [0.52 (5); Parsons *et al.*, 2013] and Hooft’s Bayesian analysis [0.51 (5); Hooft *et al.*, 2010]. All of these indicators suggest that the specimen used for the diffraction experiment was a twin. Refinement converged for a volume ratio of 0.7 (2):0.3 (2) for the twin domains.

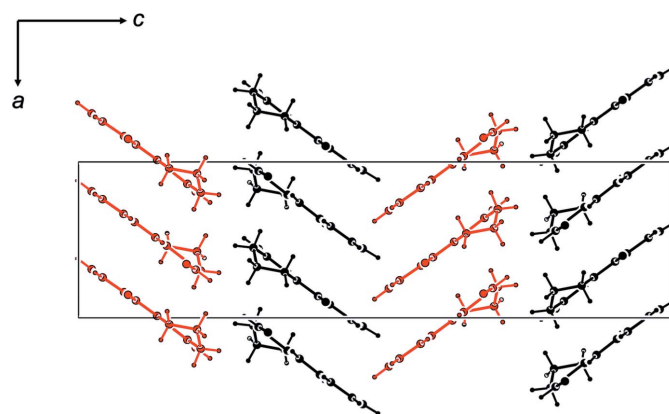


Figure 3
Packing in a view along [010]; the independent molecules *A* (black) and *B* (red) stack into separate columns of equidistant molecules along [100].

Table 1

Hydrogen-bond geometry (Å, °).

$D-H\cdots A$	$D-H$	$H\cdots A$	$D\cdots A$	$D-H\cdots A$
$N5A-H5A\cdots O2A$	0.93 (3)	1.77 (3)	2.592 (3)	146 (3)
$N5B-H5B\cdots O2B$	0.90 (3)	1.82 (3)	2.582 (3)	141 (3)
$C1A-H1A2\cdots O1A^i$	0.99	2.57	3.535 (3)	164
$C6A-H6A\cdots O1A^{ii}$	0.95	2.39	3.230 (4)	147
$C6B-H6B\cdots O1B^{ii}$	0.95	2.40	3.239 (4)	148
$C8A-H8A\cdots O1B^{iii}$	0.95	2.60	3.469 (4)	153
$C1B-H1B2\cdots O1B^{iv}$	0.99	2.59	3.550 (3)	164

Symmetry codes: (i) $x + \frac{1}{2}, -y + \frac{1}{2}, z$; (ii) $x, y + 1, z$; (iii) $-x + 1, -y + 1, z + \frac{1}{2}$; (iv) $x - \frac{1}{2}, -y + \frac{1}{2}, z$.

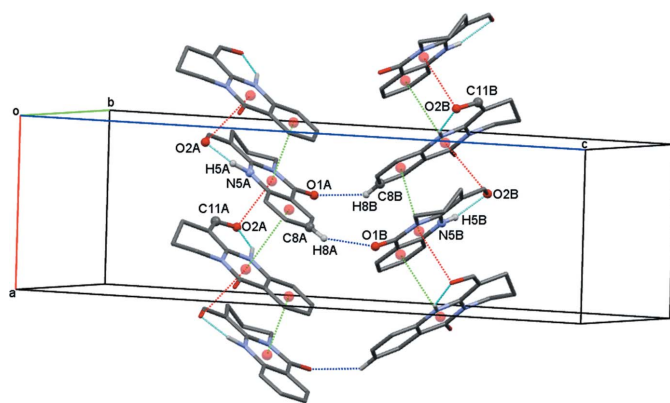
3. Supramolecular features

Consecutive molecules in each column along [100] interact *via* π - π stacking and $C=O\cdots\pi$ contacts (Fig. 4). π - π stacking interactions occur between pyrimidine ($Cg1, Cg7$) and benzene ($Cg3, Cg9$) rings and involve contact distances of $Cg1\cdots Cg3(-\frac{1}{2} + x, \frac{3}{2} - y, z) = 3.5154$ (18) Å (slippage 0.954 Å) and of $Cg7\cdots Cg9(-\frac{1}{2} + x, \frac{3}{2} - y, z) = 3.5159$ (19) Å (slippage 1.054 Å).

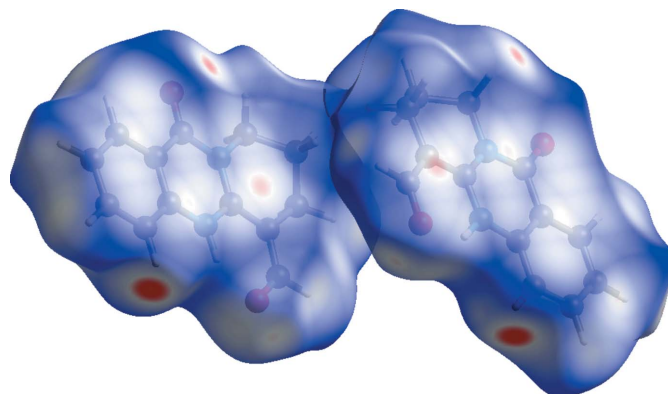
Molecules within each π -stacked column additionally interact *via* $C=O\cdots\pi$ contacts; they amount to $C11A=O2A\cdots Cg1(x + \frac{1}{2}, -y + \frac{3}{2}, z) = 3.212$ (2) Å and $C11B=O2B\cdots Cg7(x - \frac{1}{2}, -y + \frac{3}{2}, z) = 3.215$ (2) Å. Perpendicular to the stacking direction, non-classical $C-H\cdots O$ hydrogen bonds (Table 1) link the columns along [001] (Fig. 4) and thus form layers parallel to (010).

4. Hirshfeld surface analysis

In order to visualize intermolecular interactions in (**1**), the Hirshfeld surface (HS) (Spackman & Jayatilaka, 2009) was


Figure 4

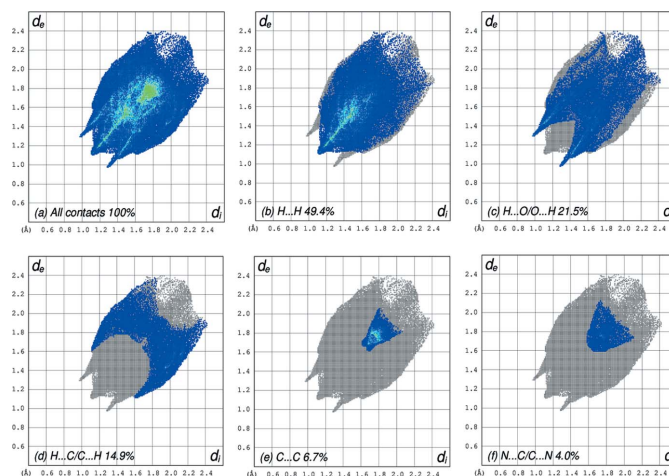
Crystal packing of (**1**) in a view along [100]. Intramolecular $N-H\cdots O$ hydrogen bonds are shown as light-blue and intermolecular $C-H\cdots O$ hydrogen bonds as dark-blue dashed lines. Dashed red lines denote contacts $C=O\cdots Cg1$ and $C=O\cdots Cg7$ (slippage 1.676 Å for both), and dashed light-green lines $Cg1\cdots Cg3$ and $Cg7\cdots Cg9$ contacts. $Cg3, Cg9, Cg1$ and $Cg7$ correspond to the ring centroids $C6A-C9A/C9AA/C5AA, C6B-C9B/C9BA/C5BA, N5A/C4AA/N10A/C10A/C9AA/C5AA$ and $N5B/C4BA/N10B/C10B/C9BA/C5BA$, respectively. For clarity, only H atoms $H5A, H8A, H5B$ and $H8B$ are shown.


Figure 5

Three-dimensional Hirshfeld surface of the title compound plotted over d_{norm} in the range -0.2446 to 1.1709 a.u.

analysed and the associated two-dimensional fingerprint plots (McKinnon *et al.*, 2007) calculated with *Crystal Explorer 17* (Turner *et al.*, 2017). The HS mapped with d_{norm} is represented in Fig. 5. White surface areas indicate contacts with distances equal to the sum of van der Waals radii, whereas red and blue colours denote distances shorter (*e.g.* due to hydrogen bonds) or longer than the sum of the van der Waals radii, respectively.

The two-dimensional fingerprint plot for all contacts is depicted in Fig. 6*a*. $H\cdots H$ contacts are responsible for the largest contribution (49.4%) to the Hirshfeld surface (Fig. 6*b*). Besides these contacts, $H\cdots O/O\cdots H$ (21.5%), $H\cdots C/C\cdots H$ (14.9%), $C\cdots C$ (6.7%) and $N\cdots C/C\cdots N$ (4.0%) interactions contribute significantly to the total Hirshfeld surface; their decomposed fingerprint plots are shown in Fig. 6*c-f*. The contributions of further contacts are only minor and amount to $N\cdots O/O\cdots N$ (1.4%), $C\cdots O/O\cdots C$ (1.4%), $N\cdots H/H\cdots N$ (0.5%) and $O\cdots O$ (0.1%).


Figure 6

Hirshfeld fingerprint plots for (a) all contacts and decomposed into (b) $H\cdots H$, (c) $H\cdots O/O\cdots H$, (d) $H\cdots C/C\cdots H$, (e) $C\cdots C$ and (f) $N\cdots C/C\cdots N$ contacts. d_i and d_e denote the closest internal and external distances (in Å) from a point on the surface.

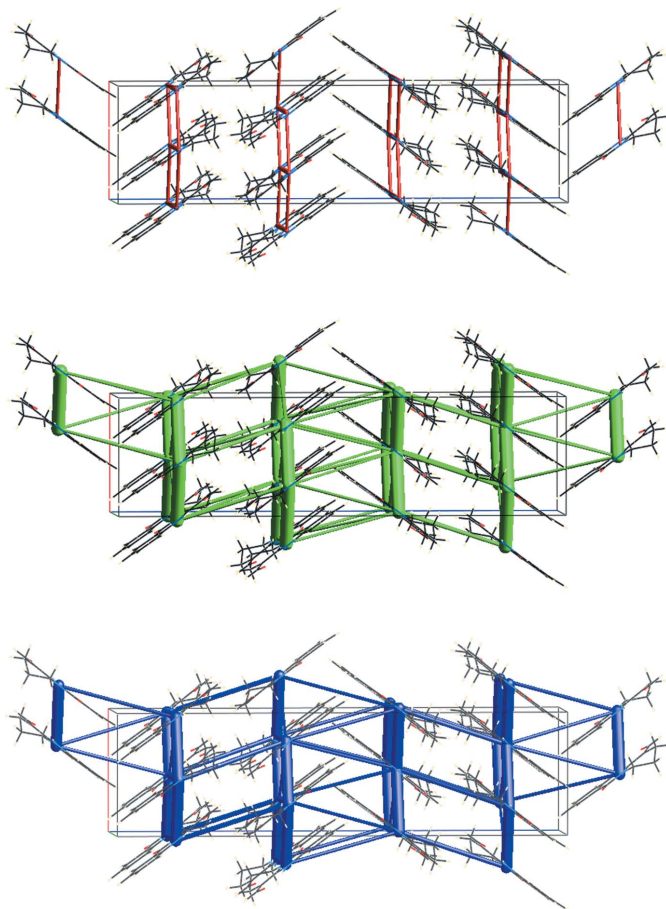


Figure 7
Energy frameworks for the electrostatic (red, top) and dispersion (green, middle) components and the total interaction energy (blue, bottom). Cylinder radii are proportional to the corresponding energy; a scale factor of 80 and a cut-off value of 10 kJ mol⁻¹ have been used.

5. Interaction energy calculations

Intermolecular interaction energies were calculated using the CE-HF/3-21G energy model available in *Crystal Explorer 17* (Turner *et al.*, 2017). The total intermolecular energy (E_{tot}) is the sum of electrostatic (E_{elec}), polarization (E_{pol}), dispersion (E_{dis}) and exchange-repulsion (E_{rep}) energies (Turner *et al.*, 2015) with scale factors of 1.019, 0.651, 0.901 and 0.811, respectively (Mackenzie *et al.*, 2017). According to these calculations, the major contribution of -306.5 kJ mol⁻¹ is due to dispersion interactions (Fig. 7). The other energy components have values of -91.5 kJ mol⁻¹, -37.6 kJ mol⁻¹ and 155.7 kJ mol⁻¹ for the E_{elec} , E_{pol} and E_{rep} energies, respectively. The total interaction energy resulting from these four components amounts to -267.1 kJ mol⁻¹.

6. Database survey

A search in the Cambridge Structural Database (CSD, version 5.41, update January 2020; Groom *et al.*, 2016) revealed six matches for molecules containing the 3-methyl-2-(propan-2-ylidene)-2,3-dihydroquinazolin-4(1*H*)-one moiety with a similar planar conformation to that in the title structure:

Table 2
Experimental details.

Crystal data	
Chemical formula	C ₁₃ H ₁₂ N ₂ O ₂
M_r	228.25
Crystal system, space group	Orthorhombic, <i>Pna</i> 2 ₁
Temperature (K)	100
a, b, c (Å)	8.284 (2), 8.006 (2), 31.637 (6)
V (Å ³)	2098.2 (8)
Z	8
Radiation type	Cu $K\alpha$
μ (mm ⁻¹)	0.81
Crystal size (mm)	0.40 × 0.22 × 0.07
Data collection	
Diffractometer	Stoe Stadivari goniometer, Dectris Pilatus 200K area detector
Absorption correction	Multi-scan (<i>LANA</i> ; Koziskova <i>et al.</i> , 2016)
$T_{\text{min}}, T_{\text{max}}$	0.261, 1.000
No. of measured, independent and observed [$I > 2\sigma(I)$] reflections	15842, 3629, 3409
R_{int}	0.013
$(\sin \theta/\lambda)_{\text{max}}$ (Å ⁻¹)	0.619
Refinement	
$R[F^2 > 2\sigma(F^2)], wR(F^2), S$	0.036, 0.103, 1.03
No. of reflections	3629
No. of parameters	316
No. of restraints	2
H-atom treatment	H atoms treated by a mixture of independent and constrained refinement
$\Delta\rho_{\text{max}}, \Delta\rho_{\text{min}}$ (e Å ⁻³)	0.36, -0.24
Absolute structure	Refined as an inversion twin.
Absolute structure parameter	0.3 (2)

Computer programs: *X-AREA* (Stoe & Cie, 2017), *SHELXT* (Sheldrick, 2015a), *SHELXL2018/3* (Sheldrick, 2015b), *PLATON* (Spek, 2020) and *pubCIF* (Westrip, 2010).

3-(2-methylphenyl)-2-(2-oxophenylethyl)-4(3*H*)-quinazolinone (FABWUA10; Duke & Codding, 1993), 3-(2-chlorophenyl)-2-[2-oxo-2-(4-pyridyl)ethyl]-4(3*H*)-quinazolinone (FABXAH10; Duke & Codding, 1993), 2-[2-oxo-2-(4-pyridyl)ethyl]-3-phenyl-4(3*H*)-quinazolinone (FABXEL10; Duke & Codding, 1993), 3-(2-methylphenyl)-2-[2-oxo-2-(4-pyridyl)ethyl]-4(3*H*)-quinazolinone (HADLAZ; Duke & Codding, 1993), 3-(4-chlorophenyl)-2-[2-oxo-2-(4-pyridyl)ethyl]-4(3*H*)-quinazolinone (HADLED; Duke & Codding, 1993) and (*E*)-2-[2-oxo-2-(thiophen-2-yl)ethylidene]-3-phenyl-2,3-dihydroquinazolin-4(1*H*)-one (SATJOP; Narra *et al.*, 2017). A search for the 2-amino-1,4,5,6-tetrahydropyridine-3-carbaldehyde moiety gave one hit with similar conformation: 1-methyl-2-(methylamino)-1,4,5,6-tetrahydropyridine-3-carbaldehyde (MFHPYM10; Horváth *et al.*, 1983). Similar to in (1), all compounds mentioned above exist as the enamine tautomer in the crystalline state, and their intramolecular N—H...O hydrogen bond between the ethanone and the amine N atom results in an *S*(6) graph set motif.

7. Synthesis and crystallization

Compound (1) was synthesized according to the method of Oripov *et al.* (1979). Yield 12.55 g, 91%; m.p. 474–476 K (after crystallization from hexane), R_f 0.78 (C₆H₆: MeOH 4:1). A

detailed report on the synthesis of (**1**) and its characterization by ^1H NMR is available in Zhurakulov *et al.* (2017). Crystals suitable for X-ray diffraction were obtained from a methanol solution by slow evaporation of the solvent at room temperature.

8. Refinement

Crystal data, data collection and structure refinement details are summarized in Table 2. H atoms attached to C were positioned geometrically, with C–H = 0.95 Å (for aromatic), 0.95 Å (for the aldehyde H atom), 0.99 Å (for methylene H atoms) and were refined with $U_{\text{iso}}(\text{H}) = 1.2U_{\text{eq}}(\text{C})$. The enamine H atoms H5A and H5B were refined with a common isotropic displacement parameter; N–H distances were restrained to similarity.

Acknowledgements

The authors are grateful to the Institute of Inorganic Chemistry, RWTH Aachen University for providing laboratory facilities.

Funding information

AT is grateful to the Istedod Foundation of the Uzbekistan Government for financial support.

References

- Duke, N. E. C. & Coddling, P. W. (1993). *Acta Cryst.* **B49**, 719–726.
- Fitzgerald, J. S., Johns, S. R., Lamberton, J. A. & Redcliffe, A. H. (1966). *Aust. J. Chem.* **19**, 151–159.
- Flack, H. D. (1983). *Acta Cryst.* **A39**, 876–881.
- Flack, H. D. & Shmueli, U. (2007). *Acta Cryst.* **A63**, 257–265.
- Groom, C. R., Bruno, I. J., Lightfoot, M. P. & Ward, S. C. (2016). *Acta Cryst.* **B72**, 171–179.
- Hooft, R. W. W., Straver, L. H. & Spek, A. L. (2010). *J. Appl. Cryst.* **43**, 665–668.
- Horváth, A., Hermecz, I., Vasvári-Debrecezy, L., Simon, K., Pongor-Csákvári, M., Mészáros, Z. & Tóth, G. (1983). *J. Chem. Soc. Perkin Trans. 1*, pp. 369–377.
- Koziskova, J., Hahn, F., Richter, J. & Kožíšek, J. (2016). *Acta Chim. Slov.* **9**, 136–140.
- Mackenzie, C. F., Spackman, P. R., Jayatilaka, D. & Spackman, M. A. (2017). *IUCrJ*, **4**, 575–587.
- McKinnon, J. J., Jayatilaka, D. & Spackman, M. A. (2007). *Chem. Commun.* pp. 3814–3816.
- Narra, S. R., Avula, S., Kuchukulla, R. R., Nanubolu, J. B., Banda, N. & Yadla, R. (2017). *Tetrahedron*, **73**, 4730–4738.
- Oripov, E., Shakhidoyatov, K. M., Kadyrov, C. S. & Abdullaev, N. D. (1979). *Chem. Heterocycl. Compd.* **15**, 556–564.
- Parsons, S., Flack, H. D. & Wagner, T. (2013). *Acta Cryst.* **B69**, 249–259.
- Shakhidoyatov, Kh. M. (1988). *Quinazol-4-ones and their Biological Activity*, p. 60. Tashkent: Fan. [In Russian]
- Shakhidoyatov, Kh. M. & Elmuradov, B. Zh. (2014). *Chem. Nat. Compd.* **50**, 781–800.
- Shakhidoyatov, K. M., Irisbaev, A., Yun, L. M., Oripov, E. & Kadyrov, C. S. (1976). *Chem. Heterocycl. Compd.* **11**, 1564–1569.
- Sheldrick, G. M. (2015a). *Acta Cryst.* **A71**, 3–8.
- Sheldrick, G. M. (2015b). *Acta Cryst.* **C71**, 3–8.
- Spackman, M. A. & Jayatilaka, D. (2009). *CrystEngComm*, **11**, 19–32.
- Spek, A. L. (2020). *Acta Cryst.* **E76**, 1–11.
- Stoe & Cie (2017). *X-Area*. Stoe & Cie GmbH, Darmstadt, Germany.
- Turner, M. J., McKinnon, J. J., Wolff, S. K., Grimwood, D. J., Spackman, P. R., Jayatilaka, D. & Spackman, M. A. (2017). *CrystalExplorer17*. University of Western Australia. <http://hirshfeldsurface.net>.
- Turner, M. J., Thomas, S. P., Shi, M. W., Jayatilaka, D. & Spackman, M. A. (2015). *Chem. Commun.* **51**, 3735–3738.
- Wang, A. & Englert, U. (2019). *Acta Cryst.* **C75**, 1448–1453.
- Westrip, S. P. (2010). *J. Appl. Cryst.* **43**, 920–925.
- Zhurakulov, Sh. N. & Vinogradova, V. I. (2015). *Uzbek Chemical Journal*, **5**, 25–29.
- Zhurakulov, Sh. N. & Vinogradova, V. I. (2016). *Int. J. Chem. Phys. Sci.* **5**, 1–7.
- Zhurakulov, Sh. N., Vinogradova, V. I. & Levkovich, M. G. (2016). *Uzbek Chemical Journal*, **4**, 75–81.
- Zhurakulov, S. N., Levkovich, M. G. & Vinogradova, V. I. (2017). *Chem. Sustainable Dev.* **25**, 265–269.

supporting information

Acta Cryst. (2021). E77, 47–51 [https://doi.org/10.1107/S2056989020016059]

Crystal structure, Hirshfeld surface analysis and energy framework study of 6-formyl-7,8,9,11-tetrahydro-5H-pyrido[2,1-b]quinazolin-11-one

Akmal Tojiboev, Sherzod Zhurakulov, Valentina Vinogradova, Ulli Englert and Ruimin Wang

Computing details

Data collection: *X-AREA* (Stoe & Cie, 2017); cell refinement: *X-AREA* (Stoe & Cie, 2017); data reduction: *X-AREA* (Stoe & Cie, 2017); program(s) used to solve structure: SHELXT (Sheldrick, 2015a); program(s) used to refine structure: *SHELXL2018/3* (Sheldrick, 2015b); molecular graphics: *PLATON* (Spek, 2020); software used to prepare material for publication: *pubCIF* (Westrip, 2010).

6-Formyl-7,8,9,11-tetrahydro-5H-pyrido[2,1-b]quinazolin-11-one

Crystal data

$C_{13}H_{12}N_2O_2$	$D_x = 1.445 \text{ Mg m}^{-3}$
$M_r = 228.25$	Cu $K\alpha$ radiation, $\lambda = 1.54186 \text{ \AA}$
Orthorhombic, <i>Pna</i> 2 ₁	Cell parameters from 17372 reflections
$a = 8.284 (2) \text{ \AA}$	$\theta = 5.6\text{--}73.9^\circ$
$b = 8.006 (2) \text{ \AA}$	$\mu = 0.81 \text{ mm}^{-1}$
$c = 31.637 (6) \text{ \AA}$	$T = 100 \text{ K}$
$V = 2098.2 (8) \text{ \AA}^3$	Plate, brown
$Z = 8$	$0.40 \times 0.22 \times 0.07 \text{ mm}$
$F(000) = 960$	

Data collection

Stoe Stadivari goniometer, Dectris Pilatus 200K area detector diffractometer	15842 measured reflections
Radiation source: XENOCs microsource	3629 independent reflections
rotation method, ω scans	3409 reflections with $I > 2\sigma(I)$
Absorption correction: multi-scan (<i>LANA</i> ; Koziskova <i>et al.</i> , 2016)	$R_{\text{int}} = 0.013$
$T_{\text{min}} = 0.261$, $T_{\text{max}} = 1.000$	$\theta_{\text{max}} = 72.8^\circ$, $\theta_{\text{min}} = 5.6^\circ$
	$h = -7 \rightarrow 10$
	$k = -7 \rightarrow 9$
	$l = -35 \rightarrow 38$

Refinement

Refinement on F^2	H atoms treated by a mixture of independent and constrained refinement
Least-squares matrix: full	$w = 1/[\sigma^2(F_o^2) + (0.0861P)^2 + 0.1201P]$
$R[F^2 > 2\sigma(F^2)] = 0.036$	where $P = (F_o^2 + 2F_c^2)/3$
$wR(F^2) = 0.103$	$(\Delta/\sigma)_{\text{max}} = 0.004$
$S = 1.03$	$\Delta\rho_{\text{max}} = 0.36 \text{ e \AA}^{-3}$
3629 reflections	$\Delta\rho_{\text{min}} = -0.24 \text{ e \AA}^{-3}$
316 parameters	Extinction correction: SHELXL-2018/3
2 restraints	(Sheldrick, 2015b),
Primary atom site location: dual	$Fc^* = kFc/[1 + 0.001xkFc^2\lambda^3/\sin(2\theta)]^{-1/4}$
Hydrogen site location: mixed	

Extinction coefficient: 0.0008 (2)

Absolute structure: Refined as an inversion
twin.

Absolute structure parameter: 0.3 (2)

Special details

Geometry. All esds (except the esd in the dihedral angle between two l.s. planes) are estimated using the full covariance matrix. The cell esds are taken into account individually in the estimation of esds in distances, angles and torsion angles; correlations between esds in cell parameters are only used when they are defined by crystal symmetry. An approximate (isotropic) treatment of cell esds is used for estimating esds involving l.s. planes.

Refinement. Refined as a two-component inversion twin

Fractional atomic coordinates and isotropic or equivalent isotropic displacement parameters (\AA^2)

	<i>x</i>	<i>y</i>	<i>z</i>	$U_{\text{iso}}^*/U_{\text{eq}}$
O1A	0.6021 (2)	0.3190 (2)	0.91582 (6)	0.0238 (4)
O2A	0.9070 (2)	0.9397 (2)	0.81869 (6)	0.0273 (4)
N10A	0.7388 (2)	0.4746 (2)	0.86753 (6)	0.0188 (4)
N5A	0.7374 (4)	0.7667 (3)	0.87182 (9)	0.0205 (6)
H5A	0.785 (4)	0.861 (3)	0.8601 (12)	0.031 (5)*
C10A	0.6394 (3)	0.4572 (3)	0.90289 (7)	0.0193 (4)
C4AA	0.7900 (3)	0.6267 (3)	0.85180 (7)	0.0183 (5)
C5AA	0.6354 (3)	0.7651 (3)	0.90621 (10)	0.0156 (6)
C9AA	0.5867 (3)	0.6135 (3)	0.92277 (9)	0.0199 (6)
C9A	0.4876 (4)	0.6078 (3)	0.95915 (9)	0.0198 (6)
H9A	0.450928	0.504197	0.970188	0.024*
C8A	0.4454 (4)	0.7578 (3)	0.97834 (12)	0.0208 (7)
H8A	0.386242	0.756350	1.004070	0.025*
C7A	0.4889 (4)	0.9111 (4)	0.96020 (9)	0.0201 (5)
H7A	0.450755	1.012023	0.972419	0.024*
C6A	0.5870 (3)	0.9174 (4)	0.92456 (9)	0.0221 (5)
H6A	0.620410	1.021297	0.912959	0.027*
C4A	0.8927 (3)	0.6410 (3)	0.81695 (8)	0.0219 (5)
C11A	0.9422 (3)	0.7999 (4)	0.80294 (8)	0.0236 (5)
H11A	1.010208	0.801898	0.778758	0.028*
C3A	0.9495 (3)	0.4844 (3)	0.79423 (7)	0.0251 (5)
H3A1	1.055458	0.449174	0.805650	0.030*
H3A2	0.962786	0.508158	0.763718	0.030*
C2A	0.8267 (3)	0.3449 (3)	0.80027 (8)	0.0261 (5)
H2A1	0.725049	0.374290	0.785613	0.031*
H2A2	0.868683	0.240345	0.787679	0.031*
C1A	0.7936 (3)	0.3181 (3)	0.84685 (7)	0.0234 (5)
H1A1	0.709624	0.231135	0.850210	0.028*
H1A2	0.893143	0.277918	0.860881	0.028*
O1B	0.6478 (2)	0.3186 (2)	0.58347 (6)	0.0246 (4)
O2B	0.3447 (2)	0.9370 (2)	0.68172 (6)	0.0260 (4)
N10B	0.5127 (2)	0.4739 (2)	0.63232 (6)	0.0182 (4)
N5B	0.5164 (4)	0.7649 (2)	0.62934 (9)	0.0175 (5)
H5B	0.482 (4)	0.861 (3)	0.6411 (12)	0.031 (5)*
C10B	0.6112 (3)	0.4574 (3)	0.59674 (7)	0.0188 (4)

C4BA	0.4630 (3)	0.6258 (3)	0.64828 (8)	0.0186 (5)
C5BA	0.6149 (4)	0.7667 (3)	0.59430 (11)	0.0206 (7)
C9BA	0.6647 (3)	0.6125 (3)	0.57672 (8)	0.0166 (5)
C9B	0.7593 (4)	0.6123 (3)	0.54056 (10)	0.0214 (6)
H9B	0.788639	0.508758	0.528072	0.026*
C8B	0.8117 (4)	0.7591 (3)	0.52233 (13)	0.0232 (8)
H8B	0.880004	0.757998	0.498217	0.028*
C7B	0.7611 (4)	0.9097 (4)	0.54040 (10)	0.0244 (6)
H7B	0.793649	1.011674	0.527607	0.029*
C6B	0.6666 (3)	0.9156 (4)	0.57585 (9)	0.0196 (5)
H6B	0.636423	1.020004	0.587748	0.023*
C4B	0.3593 (3)	0.6378 (3)	0.68323 (8)	0.0205 (5)
C11B	0.3090 (3)	0.7967 (4)	0.69727 (8)	0.0234 (4)
H11B	0.239986	0.798223	0.721255	0.028*
C3B	0.3026 (3)	0.4828 (3)	0.70566 (7)	0.0238 (5)
H3B1	0.196540	0.447861	0.694240	0.029*
H3B2	0.289541	0.506169	0.736197	0.029*
C2B	0.4255 (3)	0.3433 (3)	0.69938 (8)	0.0254 (5)
H2B1	0.527309	0.372514	0.714023	0.030*
H2B2	0.383741	0.238507	0.711861	0.030*
C1B	0.4583 (3)	0.3175 (3)	0.65270 (7)	0.0226 (5)
H1B1	0.542250	0.230628	0.649173	0.027*
H1B2	0.358647	0.277673	0.638669	0.027*

Atomic displacement parameters (\AA^2)

	U^{11}	U^{22}	U^{33}	U^{12}	U^{13}	U^{23}
O1A	0.0349 (8)	0.0136 (9)	0.0228 (8)	-0.0017 (6)	0.0023 (6)	0.0010 (5)
O2A	0.0321 (9)	0.0214 (9)	0.0282 (10)	-0.0033 (7)	-0.0001 (7)	-0.0003 (8)
N10A	0.0238 (8)	0.0142 (9)	0.0185 (9)	0.0011 (7)	-0.0015 (7)	-0.0010 (7)
N5A	0.0249 (14)	0.0170 (11)	0.0196 (13)	-0.0012 (7)	-0.0001 (11)	-0.0019 (7)
C10A	0.0225 (10)	0.0184 (11)	0.0170 (10)	0.0010 (7)	-0.0047 (8)	-0.0013 (7)
C4AA	0.0207 (10)	0.0172 (12)	0.0171 (11)	0.0013 (8)	-0.0046 (8)	0.0005 (8)
C5AA	0.0155 (14)	0.0179 (12)	0.0133 (12)	0.0008 (7)	-0.0040 (10)	0.0000 (8)
C9AA	0.0217 (12)	0.0192 (15)	0.0189 (12)	0.0017 (8)	-0.0050 (11)	-0.0019 (10)
C9A	0.0225 (12)	0.0216 (14)	0.0153 (11)	0.0016 (9)	-0.0026 (9)	0.0015 (9)
C8A	0.0249 (17)	0.0211 (16)	0.0165 (17)	0.0007 (8)	-0.0021 (11)	-0.0021 (7)
C7A	0.0251 (12)	0.0166 (12)	0.0185 (12)	0.0035 (10)	-0.0036 (10)	-0.0042 (10)
C6A	0.0246 (12)	0.0179 (13)	0.0237 (12)	0.0008 (10)	-0.0052 (11)	0.0000 (10)
C4A	0.0239 (12)	0.0204 (12)	0.0214 (12)	0.0025 (10)	-0.0023 (9)	-0.0030 (10)
C11A	0.0248 (11)	0.0254 (13)	0.0205 (12)	-0.0006 (11)	0.0001 (9)	0.0032 (11)
C3A	0.0299 (11)	0.0247 (12)	0.0208 (12)	0.0057 (9)	0.0040 (8)	0.0022 (9)
C2A	0.0370 (12)	0.0216 (10)	0.0197 (12)	0.0022 (9)	0.0011 (8)	-0.0028 (8)
C1A	0.0317 (11)	0.0180 (13)	0.0204 (13)	0.0027 (9)	0.0008 (9)	-0.0022 (8)
O1B	0.0348 (8)	0.0165 (9)	0.0226 (8)	0.0016 (6)	0.0030 (6)	-0.0001 (5)
O2B	0.0311 (8)	0.0213 (8)	0.0256 (9)	0.0023 (8)	0.0014 (6)	-0.0046 (7)
N10B	0.0237 (9)	0.0141 (9)	0.0169 (8)	-0.0007 (7)	-0.0017 (7)	0.0009 (7)
N5B	0.0209 (12)	0.0146 (11)	0.0170 (12)	0.0002 (7)	-0.0024 (10)	-0.0021 (7)

C10B	0.0228 (10)	0.0159 (10)	0.0176 (10)	0.0004 (8)	-0.0030 (8)	-0.0006 (7)
C4BA	0.0213 (10)	0.0150 (12)	0.0194 (11)	0.0006 (7)	-0.0065 (8)	-0.0005 (8)
C5BA	0.0243 (17)	0.0169 (13)	0.0205 (15)	0.0008 (8)	-0.0056 (12)	-0.0005 (9)
C9BA	0.0197 (11)	0.0139 (14)	0.0163 (11)	-0.0004 (8)	-0.0030 (10)	0.0017 (8)
C9B	0.0228 (12)	0.0178 (13)	0.0235 (13)	0.0027 (9)	-0.0029 (10)	-0.0008 (10)
C8B	0.0207 (16)	0.0280 (17)	0.0209 (19)	-0.0026 (8)	-0.0001 (11)	0.0022 (8)
C7B	0.0235 (13)	0.0231 (13)	0.0265 (14)	-0.0021 (11)	-0.0043 (11)	0.0065 (11)
C6B	0.0238 (12)	0.0144 (12)	0.0205 (12)	0.0001 (9)	-0.0038 (10)	0.0025 (9)
C4B	0.0200 (11)	0.0262 (13)	0.0154 (10)	-0.0002 (9)	-0.0031 (8)	-0.0023 (9)
C11B	0.0240 (11)	0.0261 (12)	0.0201 (12)	0.0003 (10)	-0.0019 (8)	-0.0017 (11)
C3B	0.0314 (11)	0.0215 (11)	0.0185 (11)	-0.0044 (9)	0.0031 (8)	0.0004 (8)
C2B	0.0380 (12)	0.0210 (10)	0.0170 (11)	-0.0012 (9)	0.0015 (9)	0.0035 (7)
C1B	0.0330 (11)	0.0129 (12)	0.0220 (12)	-0.0020 (8)	0.0005 (9)	0.0021 (8)

Geometric parameters (Å, °)

O1A—C10A	1.220 (3)	O1B—C10B	1.226 (3)
O2A—C11A	1.259 (4)	O2B—C11B	1.262 (4)
N10A—C4AA	1.382 (3)	N10B—C4BA	1.380 (3)
N10A—C10A	1.396 (3)	N10B—C10B	1.397 (3)
N10A—C1A	1.485 (3)	N10B—C1B	1.478 (3)
N5A—C4AA	1.359 (3)	N5B—C4BA	1.340 (3)
N5A—C5AA	1.377 (4)	N5B—C5BA	1.377 (5)
N5A—H5A	0.93 (2)	N5B—H5B	0.90 (2)
C10A—C9AA	1.467 (3)	C10B—C9BA	1.463 (3)
C4AA—C4A	1.397 (4)	C4BA—C4B	1.404 (4)
C5AA—C9AA	1.382 (4)	C5BA—C6B	1.395 (4)
C5AA—C6A	1.409 (4)	C5BA—C9BA	1.415 (4)
C9AA—C9A	1.414 (4)	C9BA—C9B	1.386 (4)
C9A—C8A	1.390 (4)	C9B—C8B	1.380 (4)
C9A—H9A	0.9500	C9B—H9B	0.9500
C8A—C7A	1.402 (4)	C8B—C7B	1.398 (4)
C8A—H8A	0.9500	C8B—H8B	0.9500
C7A—C6A	1.391 (4)	C7B—C6B	1.369 (4)
C7A—H7A	0.9500	C7B—H7B	0.9500
C6A—H6A	0.9500	C6B—H6B	0.9500
C4A—C11A	1.409 (4)	C4B—C11B	1.410 (4)
C4A—C3A	1.520 (3)	C4B—C3B	1.505 (3)
C11A—H11A	0.9500	C11B—H11B	0.9500
C3A—C2A	1.523 (3)	C3B—C2B	1.524 (3)
C3A—H3A1	0.9900	C3B—H3B1	0.9900
C3A—H3A2	0.9900	C3B—H3B2	0.9900
C2A—C1A	1.514 (3)	C2B—C1B	1.516 (3)
C2A—H2A1	0.9900	C2B—H2B1	0.9900
C2A—H2A2	0.9900	C2B—H2B2	0.9900
C1A—H1A1	0.9900	C1B—H1B1	0.9900
C1A—H1A2	0.9900	C1B—H1B2	0.9900

C4AA—N10A—C10A	123.88 (18)	C4BA—N10B—C10B	123.5 (2)
C4AA—N10A—C1A	119.42 (18)	C4BA—N10B—C1B	119.72 (19)
C10A—N10A—C1A	116.69 (17)	C10B—N10B—C1B	116.73 (18)
C4AA—N5A—C5AA	123.9 (2)	C4BA—N5B—C5BA	124.3 (2)
C4AA—N5A—H5A	110 (2)	C4BA—N5B—H5B	115 (3)
C5AA—N5A—H5A	126 (2)	C5BA—N5B—H5B	121 (3)
O1A—C10A—N10A	120.6 (2)	O1B—C10B—N10B	120.4 (2)
O1A—C10A—C9AA	123.7 (2)	O1B—C10B—C9BA	123.1 (2)
N10A—C10A—C9AA	115.7 (2)	N10B—C10B—C9BA	116.5 (2)
N5A—C4AA—N10A	117.4 (2)	N5B—C4BA—N10B	118.1 (2)
N5A—C4AA—C4A	119.7 (2)	N5B—C4BA—C4B	119.8 (2)
N10A—C4AA—C4A	122.9 (2)	N10B—C4BA—C4B	122.1 (2)
N5A—C5AA—C9AA	119.1 (2)	N5B—C5BA—C6B	121.8 (3)
N5A—C5AA—C6A	119.5 (2)	N5B—C5BA—C9BA	118.7 (2)
C9AA—C5AA—C6A	121.4 (3)	C6B—C5BA—C9BA	119.4 (3)
C5AA—C9AA—C9A	120.4 (2)	C9B—C9BA—C5BA	119.3 (2)
C5AA—C9AA—C10A	120.0 (2)	C9B—C9BA—C10B	121.8 (2)
C9A—C9AA—C10A	119.6 (2)	C5BA—C9BA—C10B	118.8 (2)
C8A—C9A—C9AA	118.3 (3)	C8B—C9B—C9BA	121.5 (3)
C8A—C9A—H9A	120.9	C8B—C9B—H9B	119.3
C9AA—C9A—H9A	120.9	C9BA—C9B—H9B	119.3
C9A—C8A—C7A	120.8 (3)	C9B—C8B—C7B	118.0 (4)
C9A—C8A—H8A	119.6	C9B—C8B—H8B	121.0
C7A—C8A—H8A	119.6	C7B—C8B—H8B	121.0
C6A—C7A—C8A	120.9 (3)	C6B—C7B—C8B	122.4 (3)
C6A—C7A—H7A	119.5	C6B—C7B—H7B	118.8
C8A—C7A—H7A	119.5	C8B—C7B—H7B	118.8
C7A—C6A—C5AA	117.9 (3)	C7B—C6B—C5BA	119.3 (3)
C7A—C6A—H6A	121.0	C7B—C6B—H6B	120.4
C5AA—C6A—H6A	121.0	C5BA—C6B—H6B	120.4
C4AA—C4A—C11A	120.0 (2)	C4BA—C4B—C11B	119.4 (2)
C4AA—C4A—C3A	119.6 (2)	C4BA—C4B—C3B	120.4 (2)
C11A—C4A—C3A	120.4 (3)	C11B—C4B—C3B	120.2 (2)
O2A—C11A—C4A	127.6 (2)	O2B—C11B—C4B	127.6 (2)
O2A—C11A—H11A	116.2	O2B—C11B—H11B	116.2
C4A—C11A—H11A	116.2	C4B—C11B—H11B	116.2
C4A—C3A—C2A	109.80 (19)	C4B—C3B—C2B	109.50 (19)
C4A—C3A—H3A1	109.7	C4B—C3B—H3B1	109.8
C2A—C3A—H3A1	109.7	C2B—C3B—H3B1	109.8
C4A—C3A—H3A2	109.7	C4B—C3B—H3B2	109.8
C2A—C3A—H3A2	109.7	C2B—C3B—H3B2	109.8
H3A1—C3A—H3A2	108.2	H3B1—C3B—H3B2	108.2
C1A—C2A—C3A	110.31 (19)	C1B—C2B—C3B	110.27 (19)
C1A—C2A—H2A1	109.6	C1B—C2B—H2B1	109.6
C3A—C2A—H2A1	109.6	C3B—C2B—H2B1	109.6
C1A—C2A—H2A2	109.6	C1B—C2B—H2B2	109.6
C3A—C2A—H2A2	109.6	C3B—C2B—H2B2	109.6
H2A1—C2A—H2A2	108.1	H2B1—C2B—H2B2	108.1

N10A—C1A—C2A	111.38 (18)	N10B—C1B—C2B	111.35 (18)
N10A—C1A—H1A1	109.4	N10B—C1B—H1B1	109.4
C2A—C1A—H1A1	109.4	C2B—C1B—H1B1	109.4
N10A—C1A—H1A2	109.4	N10B—C1B—H1B2	109.4
C2A—C1A—H1A2	109.4	C2B—C1B—H1B2	109.4
H1A1—C1A—H1A2	108.0	H1B1—C1B—H1B2	108.0
C4AA—N10A—C10A—O1A	-178.06 (19)	C4BA—N10B—C10B—O1B	-178.11 (19)
C1A—N10A—C10A—O1A	0.6 (3)	C1B—N10B—C10B—O1B	0.6 (3)
C4AA—N10A—C10A—C9AA	1.4 (3)	C4BA—N10B—C10B—C9BA	1.3 (3)
C1A—N10A—C10A—C9AA	-179.96 (19)	C1B—N10B—C10B—C9BA	-179.99 (19)
C5AA—N5A—C4AA—N10A	-0.8 (4)	C5BA—N5B—C4BA—N10B	1.5 (4)
C5AA—N5A—C4AA—C4A	179.6 (3)	C5BA—N5B—C4BA—C4B	-178.3 (3)
C10A—N10A—C4AA—N5A	-1.1 (3)	C10B—N10B—C4BA—N5B	-2.1 (3)
C1A—N10A—C4AA—N5A	-179.7 (2)	C1B—N10B—C4BA—N5B	179.2 (2)
C10A—N10A—C4AA—C4A	178.4 (2)	C10B—N10B—C4BA—C4B	177.7 (2)
C1A—N10A—C4AA—C4A	-0.2 (3)	C1B—N10B—C4BA—C4B	-1.0 (3)
C4AA—N5A—C5AA—C9AA	2.4 (4)	C4BA—N5B—C5BA—C6B	179.9 (3)
C4AA—N5A—C5AA—C6A	-179.6 (3)	C4BA—N5B—C5BA—C9BA	-0.1 (5)
N5A—C5AA—C9AA—C9A	177.3 (3)	N5B—C5BA—C9BA—C9B	177.7 (3)
C6A—C5AA—C9AA—C9A	-0.7 (5)	C6B—C5BA—C9BA—C9B	-2.3 (5)
N5A—C5AA—C9AA—C10A	-2.0 (4)	N5B—C5BA—C9BA—C10B	-0.7 (4)
C6A—C5AA—C9AA—C10A	-179.9 (2)	C6B—C5BA—C9BA—C10B	179.2 (2)
O1A—C10A—C9AA—C5AA	179.6 (2)	O1B—C10B—C9BA—C9B	1.1 (4)
N10A—C10A—C9AA—C5AA	0.2 (3)	N10B—C10B—C9BA—C9B	-178.3 (2)
O1A—C10A—C9AA—C9A	0.4 (4)	O1B—C10B—C9BA—C5BA	179.5 (2)
N10A—C10A—C9AA—C9A	-179.1 (2)	N10B—C10B—C9BA—C5BA	0.2 (3)
C5AA—C9AA—C9A—C8A	-2.0 (4)	C5BA—C9BA—C9B—C8B	2.8 (5)
C10A—C9AA—C9A—C8A	177.3 (3)	C10B—C9BA—C9B—C8B	-178.8 (3)
C9AA—C9A—C8A—C7A	5.1 (5)	C9BA—C9B—C8B—C7B	-2.6 (6)
C9A—C8A—C7A—C6A	-5.5 (5)	C9B—C8B—C7B—C6B	1.9 (6)
C8A—C7A—C6A—C5AA	2.7 (4)	C8B—C7B—C6B—C5BA	-1.5 (5)
N5A—C5AA—C6A—C7A	-177.7 (3)	N5B—C5BA—C6B—C7B	-178.4 (3)
C9AA—C5AA—C6A—C7A	0.3 (5)	C9BA—C5BA—C6B—C7B	1.7 (5)
N5A—C4AA—C4A—C11A	0.5 (4)	N5B—C4BA—C4B—C11B	1.7 (4)
N10A—C4AA—C4A—C11A	-179.0 (2)	N10B—C4BA—C4B—C11B	-178.1 (2)
N5A—C4AA—C4A—C3A	-179.2 (2)	N5B—C4BA—C4B—C3B	-178.1 (2)
N10A—C4AA—C4A—C3A	1.3 (3)	N10B—C4BA—C4B—C3B	2.1 (3)
C4AA—C4A—C11A—O2A	1.3 (4)	C4BA—C4B—C11B—O2B	0.8 (4)
C3A—C4A—C11A—O2A	-179.1 (2)	C3B—C4B—C11B—O2B	-179.4 (2)
C4AA—C4A—C3A—C2A	26.3 (3)	C4BA—C4B—C3B—C2B	26.0 (3)
C11A—C4A—C3A—C2A	-153.4 (2)	C11B—C4B—C3B—C2B	-153.9 (2)
C4A—C3A—C2A—C1A	-54.1 (3)	C4B—C3B—C2B—C1B	-54.1 (3)
C4AA—N10A—C1A—C2A	-28.9 (3)	C4BA—N10B—C1B—C2B	-28.5 (3)
C10A—N10A—C1A—C2A	152.38 (19)	C10B—N10B—C1B—C2B	152.68 (19)
C3A—C2A—C1A—N10A	56.2 (2)	C3B—C2B—C1B—N10B	56.2 (2)

Hydrogen-bond geometry (Å, °)

<i>D</i> —H \cdots <i>A</i>	<i>D</i> —H	H \cdots <i>A</i>	<i>D</i> \cdots <i>A</i>	<i>D</i> —H \cdots <i>A</i>
N5 <i>A</i> —H5 <i>A</i> \cdots O2 <i>A</i>	0.93 (3)	1.77 (3)	2.592 (3)	146 (3)
N5 <i>B</i> —H5 <i>B</i> \cdots O2 <i>B</i>	0.90 (3)	1.82 (3)	2.582 (3)	141 (3)
C1 <i>A</i> —H1 <i>A</i> 2 \cdots O1 <i>A</i> ⁱ	0.99	2.57	3.535 (3)	164
C6 <i>A</i> —H6 <i>A</i> \cdots O1 <i>A</i> ⁱⁱ	0.95	2.39	3.230 (4)	147
C6 <i>B</i> —H6 <i>B</i> \cdots O1 <i>B</i> ⁱⁱ	0.95	2.40	3.239 (4)	148
C8 <i>A</i> —H8 <i>A</i> \cdots O1 <i>B</i> ⁱⁱⁱ	0.95	2.60	3.469 (4)	153
C1 <i>B</i> —H1 <i>B</i> 2 \cdots O1 <i>B</i> ^{iv}	0.99	2.59	3.550 (3)	164

Symmetry codes: (i) $x+1/2, -y+1/2, z$; (ii) $x, y+1, z$; (iii) $-x+1, -y+1, z+1/2$; (iv) $x-1/2, -y+1/2, z$.